16.5 A CMOS Temperature-to-Frequency Converter with an Inaccuracy of ±0.5°C (3σ) from –40 to 105°C

K.A.A. Makinwa, M.F. Snoeij

Delft University of Technology, Delft, The Netherlands

This paper describes a temperature-to-frequency converter (TFC) implemented in a standard CMOS process. Its output frequency is determined by the process independent (but temperature dependent) thermal diffusivity of bulk silicon. The device-to-device spread on this frequency corresponds to an inaccuracy of less than ±0.5°C (3σ) over the extended industrial temperature range (–40 to 105°C). Unlike previous temperature sensors [1, 2], which required individual trimming to achieve this level of accuracy, this TFC only requires a simple batch calibration.

The heart of the converter is an electrothermal filter (ETF), consisting of a heater and an adjacent thermopile, realized in the substrate of a CMOS chip. As shown in Fig. 16.5.1, the heater is an n^+-diffusion resistor; while the thermopile is made from 20 p^+-diffusion/aluminum thermocouples. Power dissipation in the heater creates a local temperature gradient in the substrate, which is then sensed by the thermopile. In the thermal domain, this structure behaves like a low-pass filter, whose phase shift is determined by its geometry, and by the thermal diffusion constant D of the substrate [3]. The latter is essentially constant at the low doping levels used for the substrate and the n-well, and as such the filter's phase shift will be process independent [4]. Furthermore, since D is temperature dependent, this phase shift will be a well-defined function of temperature. Its spread will be determined mainly by the effect of lithographic inaccuracy on the distance s between the heater and the thermopile (Fig. 16.5.1). For a given process, however, such effects can be minimized by making s sufficiently large.

Since silicon is a good conductor, the temperature differences detected by the thermopile are quite small, typically being less than 0.1K at reasonable heater power levels (less than 10mW). This, in turn, results in sub-millivolt signals at the thermopile output. In combination with the thermopile's own wideband thermal noise, the result is a rather poor signal-to-noise ratio, which led to large amounts of jitter in an earlier TFC [5]. In this work, this problem has been solved by using a narrow-band tracking filter to significantly reduce the noise bandwidth.

The block diagram of the TFC is shown in Fig. 16.5.2. It is essentially a frequency-locked loop, whose main elements are an electrothermal filter, a synchronous demodulator and a voltage-controlled oscillator (VCO). The VCO drives the heater with a square-wave, which is then filtered in the thermal domain. The resulting phase-shift is detected by a synchronous demodulator consisting of a chopper and an integrator. Due to feedback, the VCO is forced to operate at the frequency f_{VCO} at which the chopper's average DC output is zero, and at which the square-wave's fundamental exhibits a fixed phase delay of about 90°. From the physics of heat diffusion, it can be shown that $f_{VCO} \propto D/s^2$ [6], and as discussed above, will be a well-defined function of temperature. The noise bandwidth of the loop is determined by the synchronous demodulator, which acts like a narrow-band filter centered on f_{VCO}.

For measurement purposes, the sub-millivolt thermopile output is boosted by a preamplifier with a nominal gain of 100. The amplifier's phase-shift, which spreads over process and temperature, should be negligible compared to that of the thermal filter. For the expected range of f_{VCO}, this requires an amplifier with a bandwidth in excess of 10MHz. To achieve this in a power efficient manner, an open-loop four-stage amplifier was implemented. Each stage consists of a PMOS transconductor and a near minimum-size PMOS diode (Fig. 16.5.3). The matching of these elements ensures that the amplifier's gain and bandwidth are sufficiently well-defined over process and temperature. A DC servo loop consisting of transconductor g_{m2} (a telescopic OTA), capacitor C_{dc} and transconductor g_{m3} (a differential pair) is used to reduce the amplifier's output offset, which would otherwise overload the synchronous demodulator. The synchronous demodulator consists of a transconductor g_{m1}, a chopper, and an external capacitor C_{ext}. For enhanced linearity, the transconductor g_{m1} (a folded-cascade OTA) employs a degenerated differential pair.

The offset of g_{m2}, typically several millivolts, will be present at the preamp output. In principle, this offset, as well as that of g_{m1} (Fig. 16.5.2), will be modulated to f_{VCO} by the chopper and then filtered out by the integrator. Due to the chopper's charge injection, however, there will be a residual offset *current* at its output. To reduce this, the thermal filter, preamp and g_{m1} are chopped at the lower frequency of $f_{VCO}/128$. This was done by adding an extra chopper (not shown) before C_{int} and modifying the phase of the heater drive such that the polarity of the demodulated thermpile output is periodically inverted.

A further source of error is cross-talk (via parasitic capacitances or the substrate) between the voltages applied to the heater and the thermopile output. The resulting spikes (Fig. 16.5.4) are in phase with the heater drive, and will give rise to a DC error signal at the output of the demodulator. To eliminate this source of error, the polarity of the heater drive is periodically inverted (at $f_{VCO}/64$). While this does not alter the generated heat, it does periodically invert the spike polarity (Fig. 16.5.4), turning it into an AC signal which will then be filtered out by the integrator.

The preamp, synchronous demodulator and two electrothermal filters were realized on a 2.3mm² chip fabricated in a standard 0.7μm CMOS process (Fig. 16.5.7). For one filter (ETF1) s = 20μm, while for the other (ETF2) s = 10μm. The on-chip electronics (excluding the heaters) dissipates 2.5mW from a 5V supply. Measurements made on 9 samples, with ETF1 operated at a heater power dissipation of 2.5mW, show that f_{VCO} has the expected $1/T^n$ dependence [5], where T is the absolute temperature in Kelvin, and n = 1.7 (Fig. 16.5.5). The spread in f_{VCO} (Fig. 16.5.6) is less than ±0.3% (3σ) over the extended industrial range (–40 to 105°C). This corresponds to an inaccuracy of less than ±0.5°C (3σ). Into a 0.5Hz bandwidth, the converter's output jitter corresponds to a noise level of about 0.04°C (rms).

References:

[1] M. Pertijs, et al., "A CMOS Temperature Sensor with a 3σ Inaccuracy of ±0.1°C from –55°C to 125°C," *ISSCC Dig. Tech. Papers,* pp. 238–239, Feb., 2005.

[2] M. Pertijs, et al., "A High-Accuracy Temperature Sensor with Second-Order Curvature Correction and Digital Bus Interface," *Proc. ISCAS*, vol. 1, pp. 368–371, May, 2001.

[3] P.R. Gray and D.J. Hamilton, "Analysis of Electrothermal Integrated Circuits," *IEEE J. Solid-State Circuits,* vol. 6, no. 1, pp. 8-14, Feb., 1971.

[4] H.R. Shanks et al., "Thermal Conductivity of Silicon from 300 to 1400K," *Physics Review*, vol. 130, 1743–1748, 1963.

[5] V. Szekely and M. Rencz, "A New Monolithic Temperature Sensor: The Thermal Feedback Oscillator," *Dig. Transducers '95*, vol. 15, pp. 849–852, June, 1995.

[6] G. Bosch, "A Thermal Oscillator Using The Thermo-Electric (Seebeck) Effect in Silicon," *Solid-State Electronics*, vol. 15, no. 8, pp. 849–852, 1972.

 1-4244-0079-1/06/$20.00

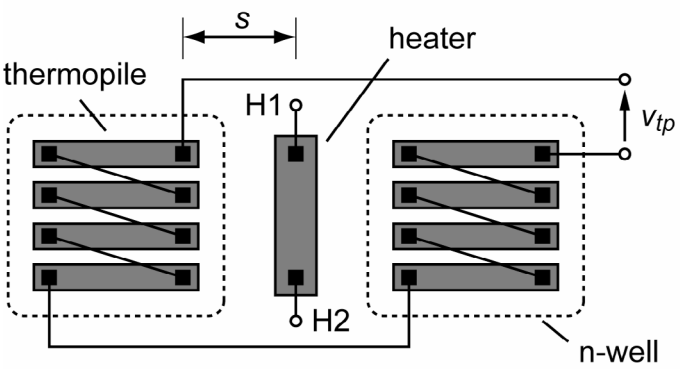

Figure 16.5.1: Schematic layout of an electrothermal filter.

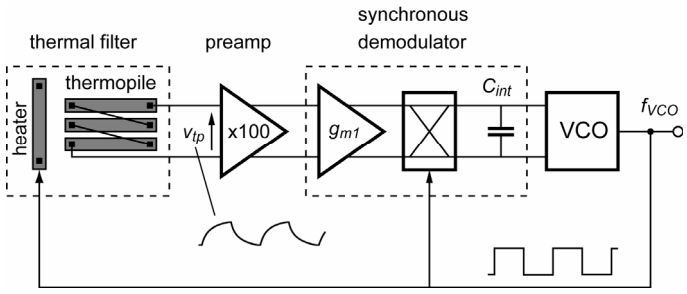

Figure 16.5.2: Block diagram of the temperature-to-frequency converter (TFC).

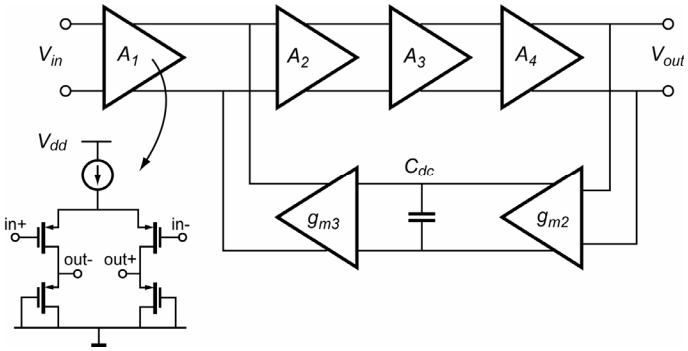

Figure 16.5.3: Thermopile preamp.

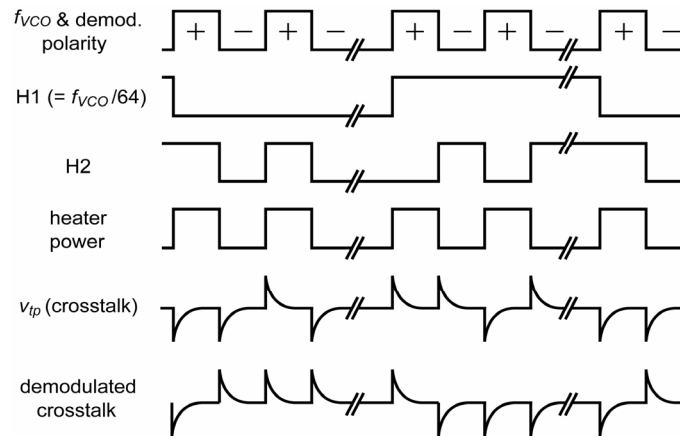

Figure 16.5.4: TFC timing diagram with heater drive inversion (HDI).

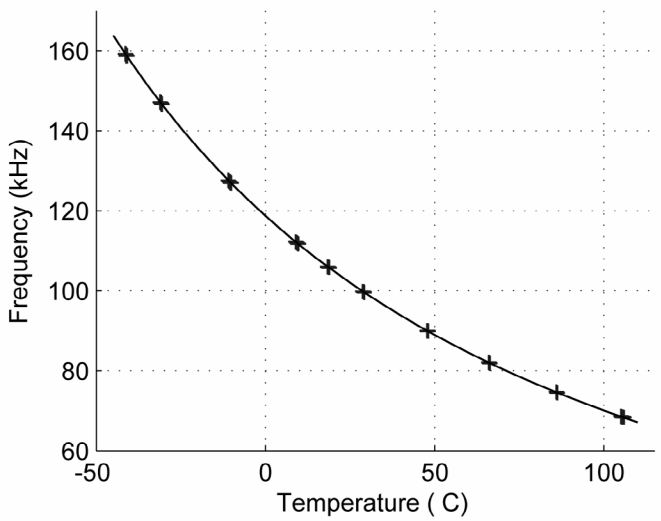

Figure 16.5.5: Measured TFC characteristic and a $1/T^n$ fit.

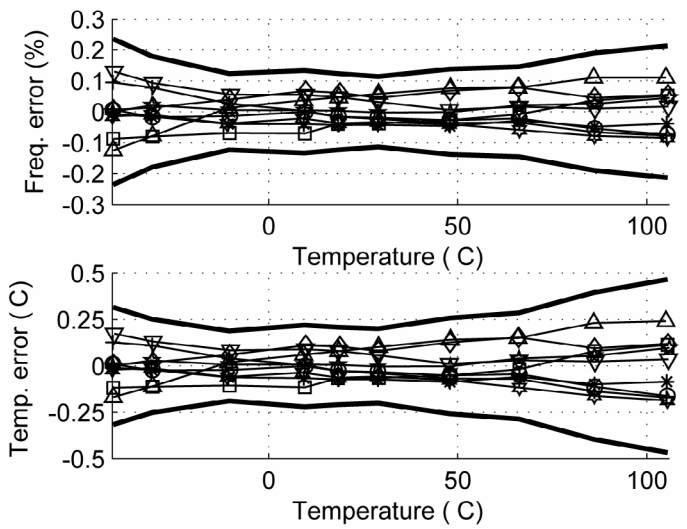

Figure 16.5.6: Measured TFC spread with ±3σ values (bold).

Continued on Page 654

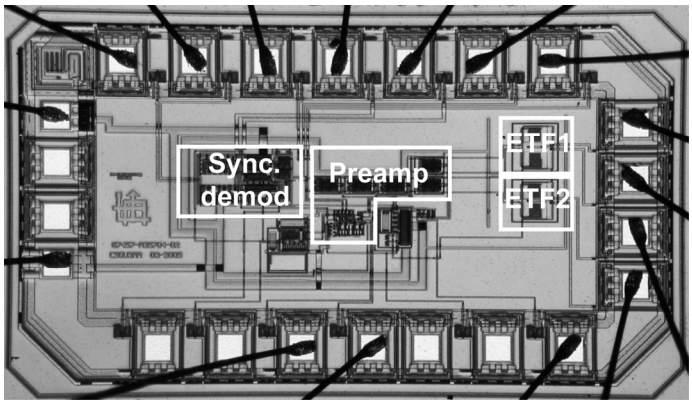

16.5.7: Chip micrograph of a temperature-to-frequency converter.

